# Modelling and Numerical Simulation of dual Fuel Lean Flames using Local Burning Velocity and critical chemical time scale

**[1]Siva PR Muppala, [2]Madhav VC Rao, [3]Naresh K. Aluri**

[1]Department of Engineering and the Environment, Kingston University London
Friars Avenue, Roehampton Vale, London, SW15 3DW, United Kingdom

[2]School of Engineering, University of Warwick
Coventry, CV4 7AL, United Kingdom

[3]General Electric, Brown-Boveri Strasse 7
5401 Baden, Switzerland

## Abstract

Addition of hydrogen to hydrocarbons in premixed turbulent combustion is of technological interest due to their increased reactivity, flame stability and extended lean extinction limits. However, such flames are a challenge to reaction modelling, especially as the strong preferential diffusion effects modify the physical processes, which are of importance even for highly turbulent high-pressure conditions. In the present work, RANS modelling is carried out to investigate pressure and hydrogen content on methane/hydrogen/air flames. For this purpose, four different subclosures, used in conjunction with an algebraic reaction model, are compared with two independent sets of experimental data: 1. Orleans data consists of pressures up to 9 bar, with addition of hydrogen content up to 20% in hydrogen/methane mixture, for moderate turbulence intensities. 2. The Paul Scherrer Institute data includes same fuels with higher volume proportion of hydrogen (40%), at much higher turbulent intensities at 5 bar. The first model Model I is based solely on the increased reactivity of the hydrogen/methane mixture under laminar conditions. It shows that the increase of unstretched laminar burning velocity ($S_{L0}$) is not sufficient to describe the increased reactivity in turbulent situations. This non-corroboration proves the importance of preferential diffusion effects in highly turbulent flames. Models II and III are formulated based on the localized increase in $S_{L0}$, local burning velocity which is a strong function of local curvature and flow strain. Model II over predicts the reactivity for higher pressures. Model III accurately predicts for nearly all studied flame conditions. Model IV is based on the leading point concept that the leading part of the turbulent flame brush is more important than rear part of premixed flame with the Lewis number less than unity. This model in its present formulation under predicts the average reaction rate compared with experiments.

*Keywords:* Turbulent premixed combustion; Hydrogen enriched flames; mean local burning velocity; Critical chemical time; multi-component flame modelling

**Nomenclature:**

| | |
|---|---|
| $b$ | Burned |
| $C_p$ | Specific heat at constant pressure (kJ/kg K) |
| $D$ | Mass diffusivity ($m^2/s$) |
| $i$ | Species |
| $I_0$ | Stretch factor |
| $Ka$ | Karlovitz number $=(u'/S_{L,0})^2 Re_t^{-1/2}$ |
| $l$ | Markstein length |
| $Le$ | Lewis number $=\alpha / D$ |
| $Le_{H_2}$ | Lewis number of hydrogen |
| $Le_{CH_4}$ | Lewis number of methane |
| $Le*$ | Effective Lewis number of the hydrogen enriched fuel mixture |
| $Ma$ | Markstein number $=l/\delta_L$ |
| $Ma_c$ | Markstein number for consumption speed |
| $Ma_d$ | Markstein number for displacement speed |
| $Ma_{h,u}$ | Markstein number for $S_{h,u}$ |
| $Re_t$ | Turbulent Reynolds number $=u'L/\nu_u$ |
| $S_{L,0}$ | Unperturbed laminar burning velocity (m/s) |
| $S_L$ | Mean local burning velocity (m/s) |
| $S_t$ | Turbulent burning velocity (m/s) |
| $\dot{}$ | Flame stretch rate |
| $T$ | Temperature (K) |
| $T_a$ | Adiabatic flame temperature (K) |
| $T_b$ | Burned temperature (K) |
| $T_u$ | Unburned temperature (K) |
| $t$ | Time (s) |
| $u$ | Unburned |
| $u'$ | RMS turbulent velocity (m/s) |
| $Ze$ | Zel'dovich number $=\beta(\gamma-1)/\gamma$ |
| $\phi$ | Equivalence ratio |
| $\rho$ | Density ($kg/m^3$) |
| $\beta$ | Normalised activation temperature $=\Theta/T_b$ |
| $\gamma$ | Gas density ratio $=\rho_u/\rho_b$ |
| $\alpha$ | Heat diffusivity ($m^2/s$) |

| | |
|---|---|
| $\tau_{cr}$ | Critical chemical time scale for highly curved flames (s) |
| $\tau_t$ | Turbulent time scale (s) |
| $\delta_L$ | Laminar flame thickness (m) $= \alpha_u / S_{L,0}$ |
| $\sigma$ | Thermal expansion coefficient |

## 1. Introduction

Lean premixed turbulent combustion has great potential in internal combustion engines, gas turbines and other combustors because of low NOx, CO and soot emissions. Under lean conditions, the flame is prone to flame instability, local extinction and blow out. A recent technique to impede such instabilities is the addition of hydrogen to the hydrocarbon fuel. This leads to increased reactivity, and extended extinction strain rate. However, the doping of hydrogen is a special challenge to the modelling of the combustion processes and of the resulting averaged turbulent reaction rate. The physical and chemical processes are significantly influenced from the highly diffusive and reactive hydrogen. Following Lipatnikov and Chomiak [1] molecular diffusion processes are not only important for laminar flame instability (e.g., thermal-diffusive instability) but also for highly turbulent flames.

Several experimental studies have been reported on the performance of hydrogen enriched fuels on knocking, emission characteristics, flame stability, extinction strain rate, lean blow out limit and burning velocity. The experiments have been carried out with different configurations such as SI engines [2], sudden expansion dump combustor [3], counter flow opposed jet [4], Bunsen [5], rod stabilized [6], freely propagating [7], spherical [8] and swirl flames [9, 10]. Systematic experiments have been carried out with a sudden expansion dump combustor by Griebel et al. [3] at high velocity and with variation of hydrogen concentration. They reported an extension of the lean blow out limit and decrease of NOx emission with addition of hydrogen into methane/air mixture. Jackson et al. [4] carried out measurements with counter flow opposed jet configuration, showing that the extinction strain rate decreases by adding hydrogen. Halter et al. [11] conducted experiments with Bunsen flame configuration and found that the flame position moves towards inlet and flame brush thickness decreases at high pressure which indicates that the flame speed increases for 10 and 20 percent hydrogen concentration in the fuel-air mixture. Law et al. [12] examined the effect of adding propane to hydrogen at different pressures and observed that propane reduces the tendency toward diffusive-thermal instability, whereas a pressure increase promotes diffusive-thermal instability, causing flame front wrinkling and high flame speeds. Schefer et al. [10] reported that the increase of hydrogen concentration at constant velocity extends the lean blow out limit and the operability range in the swirl flame. It was also mentioned that OH concentration increases in the reaction zone due to hydrogen addition especially in the positively curved edges of the flame.

Hawkes et al. [13] reported from the DNS studies of hydrogen enriched methane flames that not only OH concentration increases in the flame edges but also curvature increases for 29 %

hydrogen [13]. The increase of curvature and OH concentration increases local burning velocity which leads to increase of consumption speed (deficient reactant) in the flame. The curvature is positive when the flame front is convex towards the unburned mixture and this is considered as the leading edge of the flame, as outlined in [14]. Experimental studies by Kido et al. for single fuel [15] and multi component fuel [8] with oxidant show that the local burning velocity increases due to preferential diffusion effects. For single methane flames, the diffusivity of fuel is higher than oxygen, so methane diffuses faster than oxygen into the reaction zone. The same phenomenon occurs for multi component fuel with methane/hydrogen. Under this condition, the hydrogen diffuses faster than methane and oxygen into the reaction zone at the leading edge of the flame. This change in local stoichiometry increases the mean local burning velocity which is higher than the laminar burning velocity.

Although there exist many experimental studies on premixed turbulent hydrocarbon/hydrogen flames ([3, 5, 7, 9]), very few modelling investigations are carried out. In this study, two modelling concepts are compared for the numerical prediction of hydrogen enriched methane flames. The first approach is based on mean local burning velocities in conjunction with Markstein models. Several such approaches have been proposed for single fuel flames [16-18], two of them are selected for this study, by Bechtold and Matalon [16], and by Cant, Bray and Peters [17, 19]. In the second modelling approach of leading edge concept [1], according to Lipatnikov and Chomiak, the leading part of the turbulent flame brush is more dominant for the flame propagation. For highly turbulent conditions, typically, a critical maximum curvature can be described with a critical chemical time scale. Both approaches assume in their derivation the importance of molecular transport processes even under highly turbulent flames. The models based on a Markstein number approach should eventually be restricted to moderate turbulent situations, with an assumed linear relation between curvature or strain and local burning velocity. On the other hand, the leading edge concept based on critical curvatures should be applicable for very high turbulence situations [5]. However, this model and its limitations are not numerically explored so far.

Therefore, we investigate both types of concepts for two available sets of experiments, where amounts of hydrogen were systematically varied in methane/hydrogen mixtures, at 1 bar and higher pressures. Orléans experiments deal with methane/hydrogen Bunsen flames with turbulence characteristics in the medium range ($u'/S_L \approx 1$) with varied pressures of 1, 5 and 9 bar. The other set of experiments has been carried out with much higher turbulent flames ($u'/S_L \approx 10$) at 5 bar at the Paul-Scherrer-Institute in Switzerland. The two modelling concepts based on local burning velocity and critical chemical time scale are applied as submodels to a RANS turbulence model in conjunction with the algebraic flame surface wrinkling reaction model (AFSW) [20], which has been developed recently for lean premixed turbulent flames with increased pressure and varied fuel type. Also, with this AFSW model, we also carried out some first modelling work for methane/hydrogen mixtures with a very simple concept of an effective Lewis number [21]. However, that approach was found to be limited to 20 % hydrogen, the recent study aims to

extend the range up to 40 % hydrogen. Although the current modelling study depends in part on the reaction model, we believe, that the parts concerning the different basic concepts are to some extent independent of the underlying reaction model and should be found in similar studies in conjunction with other reaction models.

## 2. Reaction model for premixed turbulent combustion

One of the commonly proposed ways to model turbulent premixed flames is based on a reaction progress variable approach. With the strong correlation between major species and temperature, the computation of flames can be simplified essentially by describing the main reactive and thermal processes within one transport equation of the density-weighted mean reaction progress variable $\tilde{c}$ ($\tilde{c}$ = 0 in unburned and $\tilde{c}$ = 1 in burned mixtures) [22, 23].

$$\tilde{c} = \frac{T - T_u}{T_a - T_u}$$

where $T_u$ and $T_a$ are the unburned mixture and adiabatic flame temperature, respectively. The transport equation for the Favre-filtered progress variable $\tilde{c}$,

$$\frac{\partial}{\partial t}(\bar{\rho}\tilde{c}) + \frac{\partial}{\partial x_k}(\bar{\rho}\tilde{u}_k\tilde{c}) = \frac{\partial}{\partial x_k}\left(\left(\nu + \frac{\nu_t}{Sc_t}\right)\frac{\partial \tilde{c}}{\partial x_k}\right) + \dot{w}_c \qquad (1)$$

where $\bar{\rho}$ is average gas density, $\nu$ and $\nu_t$, respectively, are molecular and turbulent kinematic viscosities and the turbulent Schmidt number ($Sc_t$ = 0.7). Here the third term describes the simplified turbulent transport and the fourth term is the source term for the average reaction progress variable. The numerical scheme is based on the solution of Eq.1 in combination with the standard averaged Navier-Stokes equations [20, 22, 23].

The mean reaction rate is modelled as the product of the flame surface density $\Sigma$ per unit of flame surface area and the laminar consumption rate $\rho_u S_{L0}$:

$$\dot{w}_c = \rho_u S_{L0} I_0 \Sigma \qquad (2)$$

where unburned gas density $\rho_u$, unstretched laminar burning velocity of the fuel/air mixture $S_{L0}$, and a correction term $I_0$ for straining influence. Instead of using an additional transport equation for $\Sigma$ (e.g., [23]), we found very good results for lean methane, ethylene or propane flames with a rather simple algebraic relation for the product of a flame-surface wrinkling ratio $A_T / \bar{A}$ and the gradient of reaction progress variable (the AFSW model [20]), leading to $\dot{w}_c = \rho_u S_{L0} I_0 \frac{A_T}{\bar{A}} |\nabla \tilde{c}|$. The flame wrinkling ratio is modelled with an algebraic relation,

$$\frac{A_T}{\bar{A}} = \frac{S_T}{S_{L0}} = 1 + 0.46 \cdot Re_t^{0.25} \left( \frac{u'}{S_{L0}} \right)^{0.3} \left( \frac{p}{p_0} \right)^{0.2} \tag{3}$$

which has been parameterized to fit to an extensive set of experimental data obtained by Kobayashi et al. [24]. Here, $S_T$ is the turbulent burning velocity, turbulence is described by the turbulent Reynolds number $Re_t = u' l_x/\nu$ with turbulent rms fluctuation $u'$, turbulent length scale $l_x$, and molecular kinematic viscosity $\nu$. The explicit pressure dependent term $p/p_o$ (operating pressure over atmospheric pressure) allows comparison with experimental high-pressure flame data [20, 25]. The applicability of the AFSW model has been tested for other lean flame configurations and has also been successfully adopted as a subgrid reaction model for the LES approach [20, 26].

## 2.1 Subclosures for hydrogen doping effects:

The effects of the Lewis number and influence of pressure have been included in the reaction model and validated for three hydrocarbons with varying *Le* values and pressures up to 10 bar. However, for the hydrogen enriched flames, the preferential diffusion effects, thermo diffusive instability and increase of laminar burning velocity makes the turbulent burning velocity and reaction rate higher than in pure hydrocarbon flames.

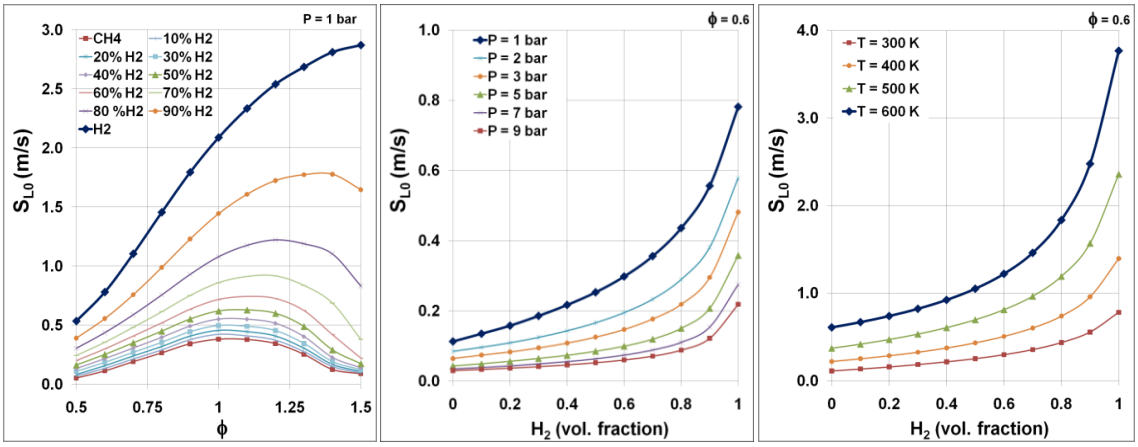


Fig. 1. Unstretched laminar burning velocity ($S_{L0}$) with variation of (from left to right) is equivalence ratio, hydrogen concentration, pressure and temperature

For laminar flames, experiments and 1-D calculations (as in Fig. 1) showed that the $S_{L0}$ increases by approximately 15 % for addition of 10 % hydrogen (by volume) to methane/air mixture. The use of this enhanced $S_{L0}$, as an input parameter however, in the turbulent combustion model, does not necessitate an equivalent increase in turbulent burning velocity compared to

experimental findings [3] [5]. We investigate this case with the reaction rate based on $S_{L0}$ (Eq.3) as Model I in this study.

In a previous study [21], we proposed a relation for an effective Lewis number, assuming the process of fuel diffusion into the flame to be similar to the weighted average of the single fuel diffusion of methane and hydrogen, leading to $D^* = x_{CH_4} D_{CH_4} + x_{H_2} D_{H_2}$, with the volume fractions $x_i$ of the fuel mixture. Accordingly, the effective Lewis number $Le^*$ of the multi fuel-mixture is expressed as

$$\frac{1}{Le^*} = \frac{D^*}{\alpha} = \frac{x_{CH_4} D_{CH_4}}{\alpha} + \frac{x_{H_2} D_{H_2}}{\alpha} = \frac{x_{CH_4}}{Le_{CH_4}} + \frac{x_{H_2}}{Le_{H_2}} \tag{4}$$

(where $\alpha$ is the thermal diffusivity of the fuel/air mixture) [21]. This very simple physical model of an average diffusivity allowed a reasonable good prediction of the same flames investigated below for the cases up to 20 % hydrogen content in conjunction with the underlying reaction model Eq. 3. However, above 20 % hydrogen this $Le^*$ approach showed deviations, and obviously this simple model is limited. Though Le includes preferential diffusion effects of hydrogen in the doped flames, the increase of curvature and stretch rate is not incorporated into the reaction model. These factors are included into the AFSW reaction model as subclosure which is based on the mean local burning velocity and critical chemical time scale.

### 2.2 Subclosure based on the mean local burning velocity

In turbulent reacting flows, local curvature and local flow strain effects modify the planar one-dimensional flame, so that the mean local burning velocity is modified in the local reaction zone. Commonly, a linear relation is assumed here for moderate curvature and flow strain effects, with the Markstein number as a phenomenological parameter and the Karlovitz number $Ka$ as dimensionless stretch parameter. We used the formulation as described in [1]:

$$S_L = S_{L0}\left(1 - Ma_c \cdot \frac{\quad}{S_{L0}}\right) \quad {}_{L0}\left(1 - Ma_c\, Ka\right) \tag{5}$$

where, $Ma_c$ is the Markstein number for consumption speed, $S_L$ is the mean local burning velocity, $S_{L0}$ is the unstretched laminar burning velocity, $\cdot \quad dt)$ is the stretch rate acting on the flame surface, owing to local curvature or locally diverging flow strain. The product of stretch rate and chemical time scale $\tau_{c0} = \delta_L / S_{L0}$ is equal to the dimensionless Karlowitz number, $Ka = \left(u'/S_{L0}\right)^2 Re_t^{-0.5}$.

The Markstein number is expressed as a phenomenological constant, being related to the physical and chemical modifications in the locally stretched flame. Some theoretical relations have been proposed for the Markstein number in the literature. We investigated two relations:
The first one is derived from theoretical asymptotic concepts from Bechtold and Matalon [16]. Without discussing the derivation, we used it in the form (in the following named as Model II):

$$Ma_c = \frac{1}{\gamma - 1}\left[\gamma ln\gamma + \frac{Ze\left(1 - Le^{-1}\right)I}{2}\right] - \frac{\gamma ln\gamma}{\gamma - 1} \tag{6a}$$

$$\text{with } I = \int_0^{\gamma-1} \frac{ln(1+x)}{x}dx \tag{6b}$$

where the Zeldovich number $Ze = (\Theta/T_b)(\gamma - 1)/\gamma$

$\gamma = \rho_u/\rho_b$ is the unburned to burned gas density ratio.

The effective Lewis number according to Eq. 4 is used as input to Eq. 6a.

We also investigated another approach by Cant, Bray and Peters [17, 19]. They assumed the modification of the local laminar burning velocity to come from either curvature or flow strain. For both, they assumed Gaussian distributions , being symmetric for the curvature with both positive and negative flame elements, and nonsymmetric for the flow strain contribution, with higher probability for positive flow strain than for negative [27]. Analyzing direct numerical simulation (DNS) studies they determined the resulting average of the laminar burning velocity. Here, the curvature effect essentially canceled out from the averaging procedure, while the flow strain effect remained physically important. According to [17, 19] (cited following [1]) the final relation for the average of the laminar burning velocity, which is termed as Model III, is

$$S_L = S_{L0}\left[1 - 0.28Ma_c\left(\psi - 0.69Ma_d\right)Ka - 0.054\,Ma_c Ma_d^2 Ka^2\psi\right] \tag{7}$$

where, $\psi = min\left\{1; exp\left[0.25\left(1 - Ka^{-0.5}\right)\right]\right\}$, and the Markstein number for displacement speed is $Ma_d = Ma_c + \frac{ln\gamma}{\gamma - 1}$. $Ma_c$ is determined in Eq. 6a.

By replacing $S_{L0}$ with $S_L$ in the reaction model, it is expected that the influence of preferential diffusion on turbulent burning velocity is captured via these Markstein number approaches. Consequently, we investigated as Model II (according to Bechtold and Matalon [16, 28]) and Model III (according to Cant, Bray and Peters [17, 19]) these relations to calculate the mean local burning velocity ($S_L$) and employed it within the algebraic flame surface wrinkling model

(Eq. 3). The modified reaction model for calculating overall turbulent burning velocity ($S_T$) is as follows

$$S_T = S_{L0} + 0.46 \cdot Re_t^{0.25} u'^{0.3} S_L^{0.7} \left( \frac{p}{p_0} \right)^{0.2} \tag{8}$$

As $S_L$ is expected to include the molecular transport effects, the *Le* term in Eq. 3 is not used in Model II and Model III.

### 2.3 Subclosure based on the leading edge concept

Kolmogorov, Petrovsky and Piskounov (KPP) analysis [29] predicts that $S_T$ is controlled by the behaviour of the mean reaction rate at the leading edge of a fully developed flame for gradient-transport turbulent diffusion. Addition of hydrogen in hydrocarbon/air mixtures with decrease in Lewis numbers (*Le*), increases the total available flame surface, and with this mechanism probably increases the overall reaction rate (view point (ii)) [30]. Betev et al. [31] pointed out a relation between the KPP-theorem and the strong Lewis number effects in premixed turbulent combustion. Both these viewpoints are correct due to equilibrium between processes (i) *within the flame brush* and (ii) *at the leading edge*. It is worth-noting that the leading point concept (LPC) is not equivalent to the KPP study. The LPC not only exploits the crucial role of the leading edge (a mathematical result by KPP), but also conjures a physical hypothesis about the structure of the leading edge [32]. The problem consists of the fact that so far this phenomenon: a very strong effect of *Le* on $S_T$ has not yet been predicted by highlighting processes *within flame brush*, while placing the focus of consideration *on the leading edge* offers an opportunity to do so. For this reason, the LPC is more appropriate for studying the preferential diffusion effects due to hydrogen on local burning velocities at the leading edges which is the subject of present investigation.

As shown in [1] and similar studies by Kido et al. [33], the highest value of the burning rate is reached in the expanding spherical flame ignited by the pocket of the critical radius if $Le < 1$. Accordingly, a critical chemical time scale $\tau_{cr}$, as defined in [21], can replace the chemical time scale $\tau_{c0}=\delta_{L0}/S_{L0}$ in the reaction closure.

The $\tau_{cr}$ as a function of Lewis number and activation temperature is described in [7] as

$$\tau_{cr} = \tau_c \, Le^{-1} \left( \frac{T_b}{T_r} \right)^{3/2} exp\left( \frac{\Theta}{2T_b} \frac{T_b - T_r}{T_r} \right); \quad T_r = T_u + (T_b - T_u)/Le \tag{9}$$

Where $T_r$ is the temperature in the critically curved flame element, $T_b$ the adiabatic flame temperature, $\Theta$ the activation temperature.

With $\tau_{cr}$ instead of $\tau_{c0}$ the modified reaction model for turbulent burning velocity ($S_T$) is

$$S_T = S_{L0} + 0.46\left(u'^{0.8} S_{L0}^{0.2}\right)\left(\frac{\tau_t}{\tau_{cr}}\right)^{1/4}\left(\frac{p}{p_0}\right)^{0.2} \tag{10}$$

where the turbulent time scale $\tau_t$ is the ratio of integral length scale $l_x$ to turbulent velocity $u'$.

## 3. Experiments and realization of the study

### 3.1 Orleans Bunsen flame

Measurements of hydrogen/methane fuel mixtures were carried out by Halter [5] in a stainless steel cylindrical combustion chamber in Orleans, France. The inlet diameter was 25 mm, the inner diameter, height and internal volume are 300, 600 mm and 80 litres, respectively. The flame was stabilized on the burner rim. Premixed lean Methane/hydrogen/air mixtures were used with hydrogen concentration in the mixed fuel varied as 0, 10 and 20-volume %, with overall equivalence ratio of the dual-fuel mixtures fixed to 0.6. The operating pressures were varied as 1, 5 and 9 bar. Turbulence was generated by a perforated plate, located 50 mm upstream the burner exit. The inlet exit hole diameter was 25 mm and it was arranged with hexagonal array. The grid mesh and blockage ratio are 2.5 mm and 0.65, respectively. The mean flow velocity at the exit of the burner was 2.1 m/s for all pressure and hydrogen variations. For cold flow, LDA measurement technique was used to predict the flow properties at the burner exit. The flame position was measured from the statistical evaluation of planar laser scattering images (Mie, Rayleigh) in the plane through the flame axis. Heat release was between 2 and 18 kW. The geometrical Reynolds numbers range between 3500 and 31500 and the turbulent Reynolds number between 33 and 329. Unstretched laminar burning velocity increases approximately by 12 % for an addition of 10 % hydrogen. In Fig. 2, the Borghi diagram shows that the atmospheric flames are situated in corrugated regime, while the high-pressure ones tend towards thin reaction regime.

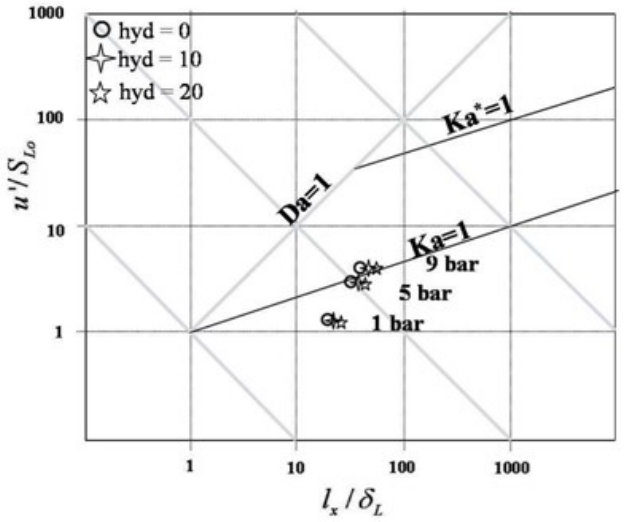


Fig. 2. Halter experimental data points marked in the Borghi diagram.

### 3.2 PSI sudden expansion dump combustor

Experiments have been conducted by Griebel et al. on a high-pressure premixed turbulent flame test rig, with methane/hydrogen/air mixtures [5]. The test was operated close to stationary gas turbine conditions. The hydrogen concentration in the fuel mixture was varied from 0 to 40% by volume and a constant overall equivalence ratio of 0.6 at 5 bar. The flame was stabilized from an outer recirculation zone coming from the sudden expansion of the combustor geometry. The length of the combustion chamber is 320 mm with the inlet nozzle diameter and expansion diameter of 25 mm and 75 mm, respectively. Inlet turbulence was generated with a turbulence grid having hexagonal pitch with hole diameter of 3 mm and blockage ration of 65%, placed 30 mm upstream of the sudden expansion. Cold flow velocity was measured with the help of 2D Particle Image Velocimetry (PIV) and the reacting field was characterized using Planar Laser Induced Fluorescence (PLIF) of the OH radical as a marker of the instantaneous flame front. The inflow geometrical and turbulent Reynolds numbers measured were about 80000 and 1000, respectively, however the latter reaches about 2300 in the shear flow region (at $x/d$ = 7). The unstretched laminar flame speed for the preheated mixture at 5 bar with 0, 10, 20, 30 and 40 % hydrogen is 0.237, 0.266, 0.296, 0.321 and 0.351 m/s, respectively. As shown in Fig. 3, the Borghi diagram projects that all the experimental data fall into the corrugated flame regime. The heat release was with about 75 kW much higher than in the Orléans Bunsen cases, and also the turbulence intensity was 10 to 20 times higher than the $S_{L0}$, so that these experiments describe highly turbulent flames.

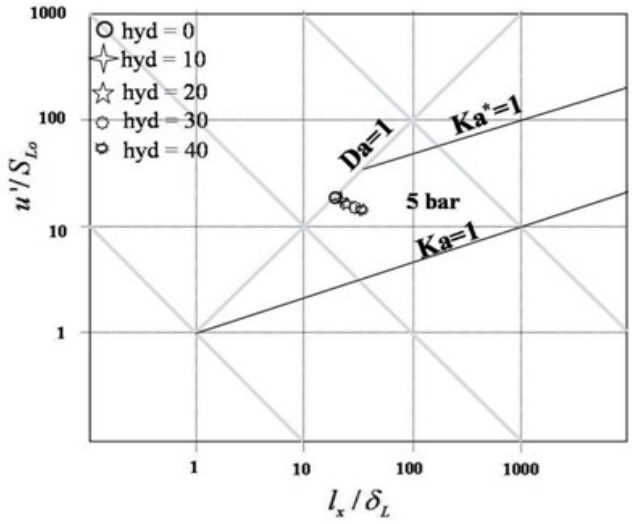


Fig. 3. PSI experimental data plotted on the Borghi diagram.

### 3.3 Numerical Implementation

For the current study, the simulations are carried out in FLUENT with two-dimensional symmetric boundary condition. Boundary conditions are determined according to the experimental data (see §3.2). Standard *k-e* model with default model constants was used for turbulence modelling. Fluent is a control-volume based solver and the transport equations are discretized such that all physical quantities are conserved on a control volume basis.

In this numerical study, two-dimensional simulations are carried out for the two simple flame configurations. The Reynolds-averaged Navier-Stokes (RANS) equations for mass, momentum and turbulence along with a scalar equation representing reaction processes are solved to handle turbulent reacting flows on an incompressible variable density solver, in the commercial software Fluent [34].

In ensemble averaging for non-density flows the solution variable are decomposed into mean and fluctuating components.

$$u_i = \bar{u}_i + u_i' \text{, for } = 1,23.$$

Pressure and scalar quantities follow this suit.

In Favre-averaged quantities, the continuity equation

$$\frac{\partial \bar{\rho}}{\partial t} + \frac{\partial}{\partial x_i} \bar{\rho} \tilde{i}$$

and

momentum equation

$$\frac{\partial \bar{\rho} \tilde{i}}{\partial t} + \frac{\partial}{\partial x_j} = \frac{}{\partial x_j} - \frac{\partial p}{\partial x_i} - \frac{\partial \tau_{ij}}{\partial x_j}$$

where $\sigma_{ij}$ is stress tensor,

$$\sigma_{ij} = -\mu\left(\frac{\partial \tilde{u}_i}{\partial x_j} + \frac{\partial \tilde{u}_j}{\partial x_i}\right) + \sigma_{ij}\frac{2}{3}\mu\frac{\partial \tilde{u}_k}{\partial x_k}$$

and, $\tau_{ij} = \widetilde{u_i u_j}$ are the Reynolds stresses (not expanded here).

The Favre-averaged turbulence quantities $\tilde{k}$ and $\varepsilon$ are modelled with the $\tilde{k}$ $\varepsilon$ turbulence model, and its performance is predictable with sufficient accuracy for these combusting flows.
The standard k-e turbulence model is used in this study, with the transport equations of turbulent kinetic energy and dissipation rate (both terms function of turbulent velocity and length scale):

$$\frac{\partial \bar{\rho} k}{\partial t} + \frac{\partial\left(\bar{\rho} u_j\right)}{\partial x_j} = \frac{\partial}{\partial x_j}\left[\left(\frac{\bar{\rho}\nu_t}{\sigma_k}\right)\frac{\partial k}{\partial x_j}\right] + G_k + G_b - \bar{\rho}\varepsilon$$

and

$$\frac{\partial \bar{\rho}\varepsilon}{\partial t} + \frac{\partial\left(\bar{\rho}\varepsilon u_j\right)}{\partial x_j} = \frac{\partial}{\partial x_j}\left[\left(\frac{\bar{\rho}\nu_t}{\sigma_k}\right)\frac{\partial \varepsilon}{\partial x_j}\right] + C_{1\varepsilon}\frac{\varepsilon}{k}\left(G_k + C_{1\varepsilon}G_b\right) - C_{2\varepsilon}\bar{\rho}\frac{\varepsilon^2}{k}$$

with constants $C_{1\varepsilon}$=1.44, $C_{2\varepsilon}$=1.92 and $C_{\mu}$=0.09. We found these original constants have been applicable for these numerical flows.
The pressure-velocity coupling is based on the SIMPLE scheme and the second-order discretization schemes are applied to all transport equations. These details are summarized below.

| | |
|---|---|
| Turbulence model | Standard $k-\varepsilon$ model |
| Pressure | II-order |
| Momentum | II-order upwind |
| Pressure-velocity coupling | SIMPLE |
| Turbulent kinetic energy and turbulent dissipation rate | II-order upwind |
| Progress variable | II-order upwind |
| Grid spacing | 0.25 mm |
| Cell count | 45,000 |

Initial and boundary conditions are set up in accordance with the experiments performed by Halter et al. [5] and by Griebel et al. [3]. The algebraic flame surface wrinkling (AFSW) reaction closure is implemented as a user-defined subroutine function to the solver. For the Bunsen flame configuration, in a pre-study both calculated flame position and flame angle are found to remain unaffected for lateral dimension equal to or greater than 40 percent of the experimental chamber diameter. Therefore, the present computations are performed for half the original diameter to reduce the computational time. Moreover, in a grid dependency test, the minimum computational

mesh size for which the flame height is not affected is 0.25 mm. For the PSI burner, the computational domain size is identical to the experimental dimensions.

## 4. Results and Discussions

In the following, RANS simulations of premixed turbulent flames for two configurations are presented using the basic AFSW reaction model and its three modified subclosures. The investigated models are named as follows

- Model I: The basic reaction model with $S_{L0}$, which does not account for preferential-thermo-diffusive instabilities, Eq. 3
- Model II: Modified $S_{L0}$ model according to Bechtold and Matalon, Eq. 6
- Model III: Modified $S_{L0}$ model according to Bray, Cant, Peters, Eq. 7
- Model IV: Leading edge model with critical curvature and critical chemical time scale, Eq. 10

Data of $S_{L0}$ have been taken from [3, 5]. The mean local burning velocity ($S_L$), the Markstein numbers and the critical chemical time scale ($\tau_{cr}$) are calculated as described before for the two sets of experimental data. In Eq. 6b, the effective Lewis number ($Le^*$) of the fuel-mixture is obtained via Eq. 4 [21] leading to values of 0.955, 0.777, 0.655, 0.566 and 0.498 for 0, 10, 20, 30 and 40 % hydrogen in methane, respectively. The activation temperatures of the mixtures are calculated with the linear mole-fraction-weighted interpolation of the activation temperatures 19000 K and 13000 K of methane and hydrogen, respectively.

### 4.1 Results of the calculated Orleans Bunsen flame

Figure 4 shows the calculated values of the mean local burning velocity normalized by unstretched laminar burning velocity $S_L/S_{L0}$ for the methane/hydrogen/air mixtures. As shown, $S_L$ reaches up to three times the value of $S_{L0}$ in Model II and two times for Model III. While for Model II the estimated Markstein number, $Ma_c$ decreases from –0.12 to –1.28, the same quantity shows a sign change from +0.24 to –0.91 for model III, from 0 to 20 % hydrogen addition as in Table I. Negative Markstein numbers describe diffusive thermal instability with increase of the local curvature and burning velocity.

In Figures 5, 6 and 7 the simulation results from the Models I to IV are shown in comparison with the experiments. While in Figure 7 some examples of the flame contours are shown directly for the 5 bar cases, it is convenient to discuss the simulated flame length in terms of a turbulent burning velocity $S_T$, in compact form normalized as $S_T/S_{L0}$ as a function of $u'/S_{L0}$ (Fig. 6). The velocity $S_T$ is here determined with the simplified relation $sin(\alpha/2) = S_T/U$, where U is the inlet

velocity and $\alpha$ is the flame cone angle. The flame angle is estimated from the flame shape of the $\bar{c} = 0.5$ contour line being considered as a triangle with the full cone angle $\alpha$ at the flame tip. The flame length is calculated by distance from inlet to $\bar{c} = 0.5$. From Figures 5 and 6, it can be seen that the purely chemical effect of increased reactivity of the added hydrogen (Model I, with increased $S_{L0}$) does not explain the experimentally observed increase of the ratio $S_T/S_{L0}$. Model II shows good agreement for pure methane/air mixtures, but it strongly deviates for higher pressures and addition of hydrogen, predicting too high reactivity. The predictions of Model III (based on Markstein numbers determined according to Cant, Bray and Peters) reached a very good agreement for 1 and 5 bar and show a slight over prediction at 9 bar and high $u'/S_{L0}$.

Table I: Calculated Markstein number and mean local burning velocity, presented for Orleans Bunsen flame experimental data

| Pressure (bar) | $H_2$ (%) | Ma (Model II) | Ma (Model III) | $S_L$ (Model II) (m/s) | $S_L$ (Model III) (m/s) |
|---|---|---|---|---|---|
| 1 | 0 | -0.1297 | 0.2454 | 0.118 | 0.113 |
| | 10 | -0.7458 | -0.3715 | 0.152 | 0.132 |
| | 20 | -1.2874 | -0.9140 | 0.181 | 0.155 |
| 5 | 0 | -0.1295 | 0.2454 | 0.049 | 0.043 |
| | 10 | -0.7449 | -0.3707 | 0.086 | 0.059 |
| | 20 | -1.2874 | -0.9140 | 0.114 | 0.082 |
| 9 | 0 | -0.1295 | 0.2454 | 0.037 | 0.031 |
| | 10 | -0.7449 | -0.3707 | 0.074 | 0.047 |
| | 20 | -1.2874 | -0.9140 | 0.103 | 0.07 |

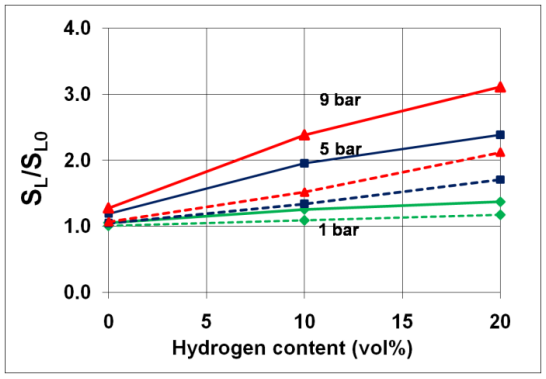


Fig. 4. Simulated normalized mean local burning velocity $S_L/S_{L0}$ for variation of hydrogen concentration and pressure variation. Solid lines – Model II, dashed lines – Model III.

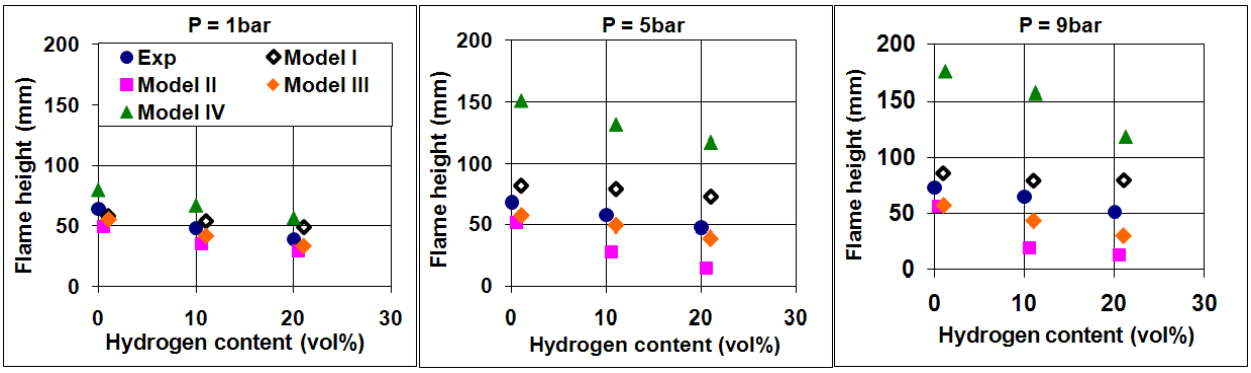


Fig. 5. Simulated and measured Bunsen flame height ($\bar{c} = 0.5$) comparison for 0, 10 and 20 % hydrogen concentration and 1, 5 and 9 bar pressure

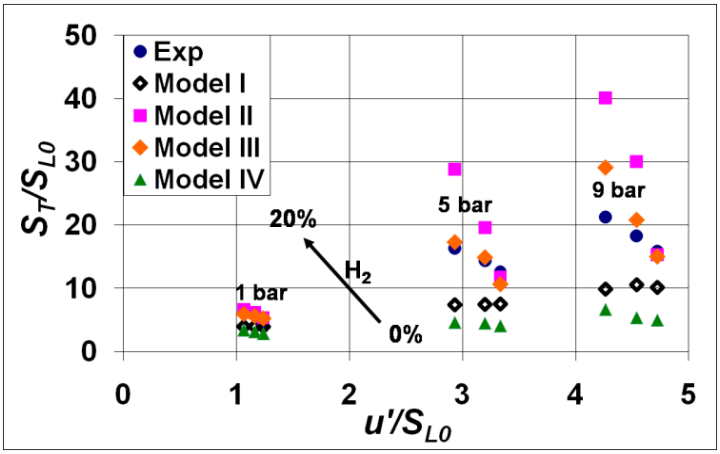


Fig. 6. Simulated and measured turbulent burning velocity normalized by unstretched laminar burning velocity $S_T/S_{L0}$ for 0, 10 and 20% hydrogen addition

For Model IV however, the quantity $S_T$ is strongly underestimated (which means that the predicted flames are much longer than the experimentally observed flames, see Fig. 7). As discussed in [1, 31], for the expanding spherical flames of *Le* <1 mixtures, at critical radius of ignition ($r_{cr}$) the consumption speed attains the maximum value. Lipatnikov and Chomiak [1, 31], showed that under such conditions, the observed ratio critical/chemical time scale ($\tau_{cr}/\tau_c$) is in the order of 0.05 for ultra-lean hydrogen/air flames. For this Bunsen flame experimental conditions, the calculated $\tau_{cr}/\tau_c$ values from Eq. 9 are 0.35 and 0.18 for 10 and 20 % $H_2$ addition. Although this general decreasing trend of $\tau_{cr}/\tau_c$ indicates that the burning rate of methane/hydrogen/air mixtures increases with hydrogen addition, the simulations under predicts $S_T$. Improved numerical predictions for this data are possible from Model IV if $\tau_{cr}$ may be obtained from the simulation of critically curved laminar flames invoking a detailed chemical kinetic mechanism [31].

To summarise for the Bunsen flame study, for measured low inlet mean velocity and turbulence conditions, the Model I shows a qualitative trend of decreasing flame shape with hydrogen

addition but it quantitatively under predicts this effect. Model II and Model IV either over predicts or under predicts the flame length for increasing concentration. Model III shows good agreement for all nine cases.

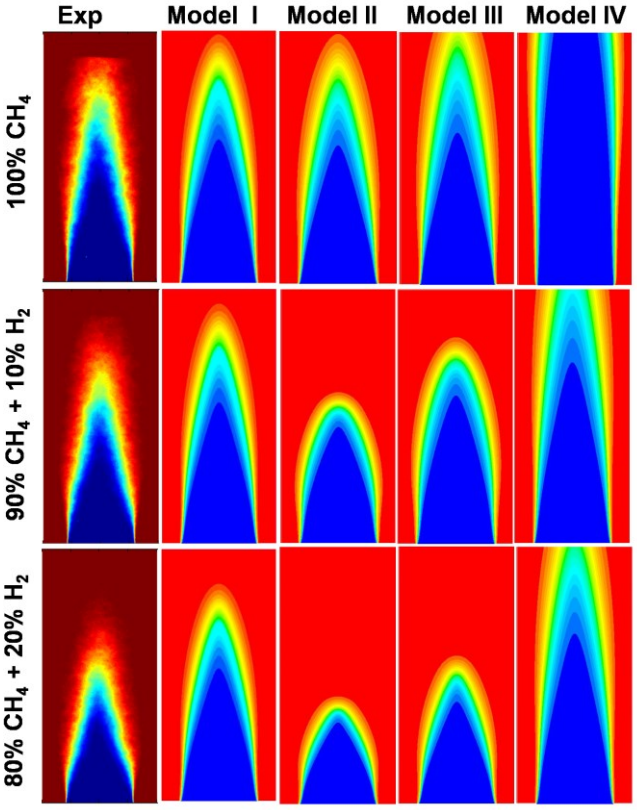


Fig. 7. Orléans Bunsen flame contours. Shown are the three cases at 5 bar pressure with 0, 10 and 20% hydrogen in methane. Left the experimental flame, followed by the simulated flames with Models I to IV. The contour values (mean reaction progress) range from 0 (blue-unburned) to 1 (red-burned).

### 4.2 Results of the highly turbulent test cases (PSI flames)

For the preheated methane/hydrogen/air mixtures, the Markstein number values from Model II and Model III lies between –0.12 and –2.13 and between +0.46 and –1.54, for 0 to 40 % hydrogen addition, respectively, as shown in Table. II. According to these effects, it can be assumed that flame instability increases for higher hydrogen concentration leading to higher burning rates. The calculated $S_L/S_{L0}$ values rise to about 3.3 for Model II and to about 4.1 for Model III, as presented in Fig. 8. The corresponding chemical time scale $\tau_{cr}/\tau_c$ values are calculated between 0.86 for pure methane and 0.17 for 40 % hydrogen, resepctively.

Table II: Calculated Markstein number and mean local burning velocity, presented for PSI experimental data

| $H_2$ | Ma | Ma | $S_L$ | $S_L$ | Critical chemical time |
|---|---|---|---|---|---|

| (%) | (Model II) | (Model III) | (Model II) (m/s) | (Model III) (m/s) | scale (Model IV) ($\tau_{cr}$)(s) |
|---|---|---|---|---|---|
| 0 | -0.1285 | 0.4627 | 0.341 | 0.267 | 0.000238 |
| 10 | -0.7203 | -0.1300 | 0.758 | 0.417 | 0.000204 |
| 20 | -1.2788 | -0.6894 | 1.084 | 0.663 | 0.000165 |
| 30 | -1.7399 | -1.1524 | 1.307 | 0.941 | 0.00014 |
| 40 | -2.1300 | -1.5440 | 1.455 | 1.199 | 0.000117 |

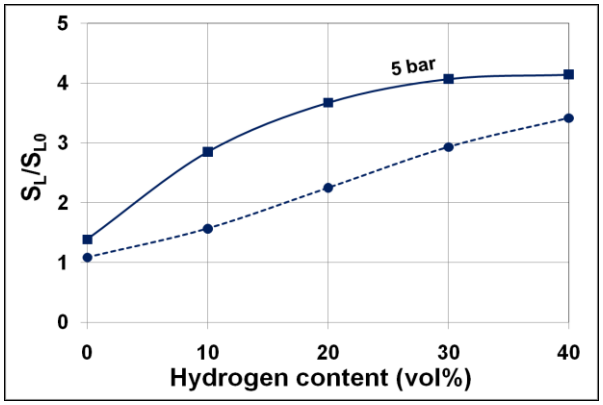


Fig. 8. The calculated normalized local burning velocity for variation of hydrogen concentration and 5 bar pressure, solid lines – Model II, dashed lines – Model III.

Figures 9 and 10 shows the experimental flame height and turbulent burning velocity (absolute value) in comparison with the calculated ones for the highly turbulent experiments at 5 bar with varied hydrogen content up to 40 %.

The basic Model I numerically predicts the flame shape satisfactorily up to 10 % hydrogen with experiments. For higher levels of turbulence and increased hydrogen doping, the Model I again completely under predicts the reactivity. This indicates that even at high turbulent conditions the molecular preferential diffusion and thermo diffusive instability effects are important and are especially noticeable for flames with increased amount of added hydrogen. As shown in Figure 10, again the Model III predictions of turbulent burning velocity are in good agreement with the experimental trend, while Model II and Model IV under predict or over predict the reactivity for all studied cases. The corresponding calculated and measured flame contours are shown in Fig. 11. Here again increased hydrogen content leads to increased reactivity, which leads to shortened flames.

Comparing the two investigated models based on the Markstein number approaches this study shows very good predictability for the relations from Cant, Bray and Peters (Model III), while the older ones (Model II) deviate by up to 50 percent. This difference is stemming from the fact

that for Model III already a fitting procedure to DNS studies has been involved which was not the case for the Model II relation.

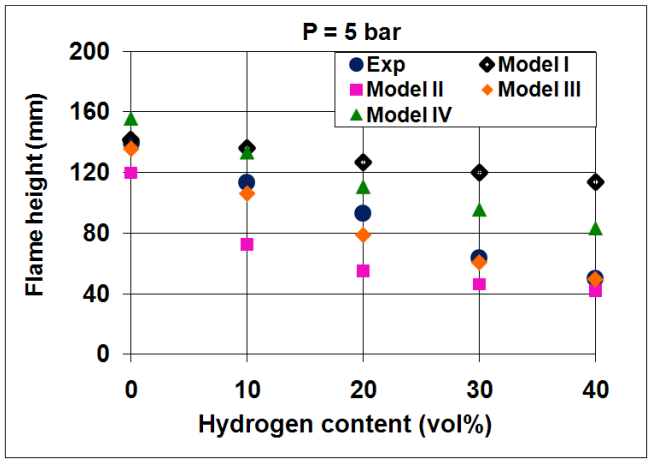


Fig. 9. Simulated and measured flame height ($\bar{c} = 0.5$) from the three subclosures are compared with PSI experimental data for 0 to 40 vol% hydrogen.

The Model IV based on the critically curved laminar flames again under predicts the reactivity significantly at much higher turbulence intensity than in the Bunsen cases. Lipatnikov and Chomiak have assumed this model to be eventually more suited for higher turbulence conditions. On the other hand they have argued that the Markstein models with a linear relation between $S_L$ and $S_{L0}$ should be valid only for small deviations of these two quantities, while in the second test case the ratio was found to be much above one. Nevertheless, the present results showed that the Model III worked well here even for high turbulence.

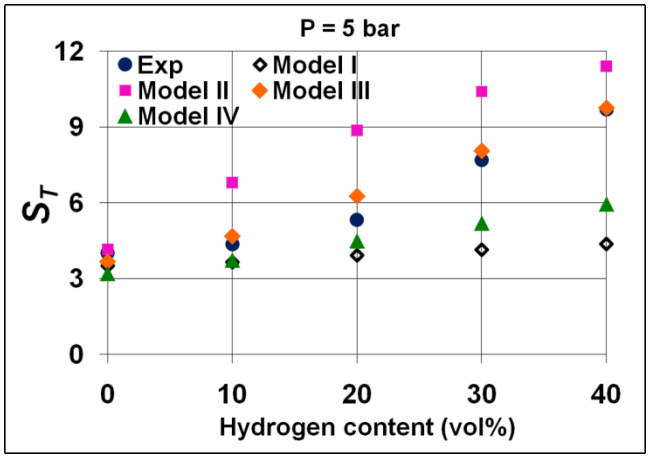


Fig. 10. Simulated turbulent burning velocities from the three subclosures are compared with PSI experimental data for 0 to 40 vol% hydrogen.

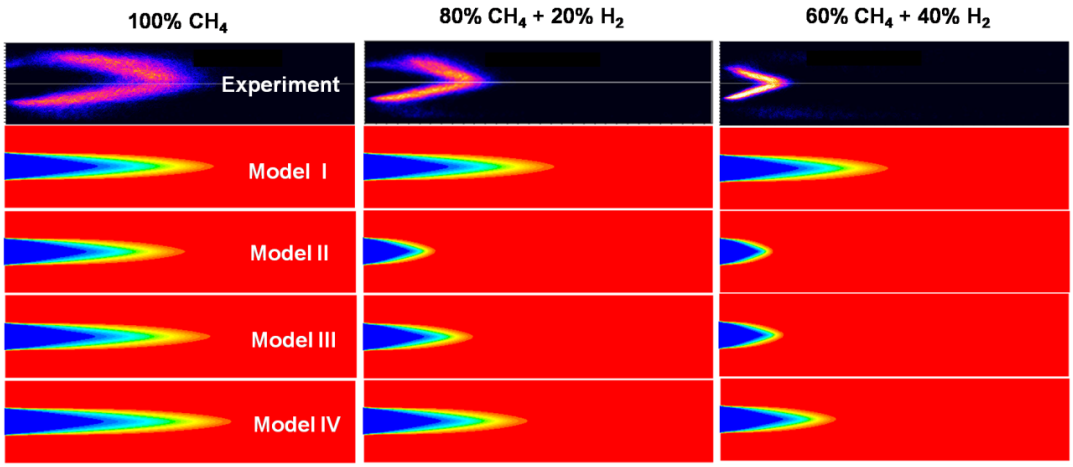


Fig. 11. PSI test flames. Simulated premixed turbulent methane/hydrogen/air flames in Reynolds-averaged reaction progress contours from the AFSW reaction model with the four Models I, II, III and IV, are shown in comparison with the measured flames, for 0, 20 and 40 % hydrogen at 5 bar. The contour values range between 0 (blue-unburned) and 1 (red-burned).

## Conclusion

Hydrogen addition to hydrocarbon fuel increases the local reaction rate at the leading edge due to preferential diffusion and Lewis number effects. In this study, two modeling concepts are considered for the prediction of hydrogen enriched methane flame and the results are compared with Bunsen and high-pressure test rig flame configurations at moderate and high turbulent conditions. The first approach is based on mean local burning velocity in conjunction with Markstein models. Several such approaches have been proposed for single fuel flames, two of them are selected for this study, by Bechtold and Matalon, and by Bray, Cant and Peters. The second modeling approach is a leading edge concept, which according to Lipatnikov and Chomiak is based on the idea that the leading part of the turbulent flame brush is more dominant for the flame propagation (and thus on the averaged reaction rate) and that for high turbulent situations typically a critical maximum curvature is of relevance, which can be described with a critical chemical time scale.

Simulations were carried out with different subclosures in conjunction with an algebraic reaction model. Model I is based solely on the increased laminar unstrained burning velocity for added hydrogen. It is not sufficient to describe the more increased reactivity in turbulent situations and thus proves the influence of preferential diffusion. Models II and III are based on two Markstein models where the local burning velocity is assumed to be modified by the local curvature and flow strain. The approach by Bechtold and Matalon (Model II) over predicts for both experimental conditions. The approach by Cant, Bray and Peters (Model III) reached good to very good quantitative agreement with both sets of data. The leading edge approach (Model

IV) gave noticeable under predictions with both measured data. These under predictions are possibly resulting from the simplified assumptions made in the estimation of the critical chemical time scale.

**References**


1. Lipatnikov, A. N. and Chomiak, J., *Molecular Transport Effects on Turbulent Flame Propagation and Structure.* Progress in Energy and Combustion Science, 2005. 31: p. 1-73.
2. Blarigan, P. V. and Keller, J. O., *A hydrogen fuelled internal combustion engine designed for single speed/power operation.* Int. J. Hydrogen Energy, 2002. 23(7): p. 603-609.
3. Griebel, P., Boschek, E., and Jansohn, P., *Flame stability and NOx emission improvements due to H2 enrichment of turbulent, lean premixed, high-pressure, methane/air flames*, in *The future of gas turbine technology*. 2006: Brussel, Belgium.
4. Jackson, G. S., Sai, R., Plaia, J. M., Boggs, C. M., and Kiger, K. T., *Erratum to "influence of H2 on the response of lean premixed CH4 flames to high strained flows"*Combust. Flame 132(3)(2003)503-511.* Combustion and Flame, 2003. 135(3): p. 363.
5. Halter, F., *Caractérisation des effets de l'ajout d'hydrogène et de la haute pression dans les flammes turbulentes de prémélange méthane/air*, in *Energétique - Mécanique des fluides*. 2005, l'Universite d'Orleans: Orleans (France). p. 1-251.
6. Lafay, Y., Renou, B., Cabot, C., and Boukahlfa, M., *Experimental and numerical investigation of the effect of H2 enrichment on laminar methane-air flame thickness.* Combustion and Flame, 2008. 153: p. 540-561.
7. Shy, S. S., Chen, Y. C., Yang, C. H., Liu, C. C., and Huang, C. M., *Effects of H2 or CO2 addition, equivalence ratio, and turbulent straining on turbulent burning velocities for lean premixed methane combustion.* Combustion and Flame, 2008. 153: p. 510-524.
8. Kido, H., Nakahara, M., Hashimoto, J., and Barat, D., *Turbulent Burning Velocities of Two-component Fuel Mixtures of Methane, Propane and Hydrogen.* JSME International Journal, Series B, 2002. 45(2).
9. Cheng, R. K., Littlejohn, D., Strakey, P. A., and Sidwell, T., *Laboratory investigations of a low-swirl injector with H2 and CH4 at gas turbine conditions.* Proceedings of the Combustion Institute, 2009. 32(2): p. 3001-3009.
10. Schäfer, R. W. *Combustion of hydrogen-enriched methane in a lean premixed swirl burner*. in *DOE Hydrogen program review*. 2001.
11. Halter, F., Cohé, C., Chauveau, C., and Gökalp, I. *Characterization of the effects of hydrogen addition in lean premixed methane/air turbulent flames at high pressure*. in *Proceedings of the European Combustion Meeting*. 2003. Orleans (France).
12. Law, C. K., Jomaas, G., and Bechtold, J. K., *Cellular instabilities of expanding hydrogen/propane spherical flames at elevated pressure: theory and experiment.* Proceeding of the combustion institute, 2005. 30: p. 159-167.
13. Hawkes, E. R. and Chen, J. H., *Direct numerical simulation of hydrogen-enriched lean premixed methane-air flames.* Combustion and Flame, 2004. 138(3): p. 242-258.
14. Lipatnikov, A. and Chomiak, J., *A theoretical study of premixed turbulent flame development.* Proceedings of the Combustion Institute, 2005. 30: p. 843.

15. Kido, H., Nakashima, K., Nakahara, M., and Hashimoto, J., *Experimental study on the configuation and propagation characteristics of premixed turbulent flame.* JSME International Journal, 2001. 22: p. 131-138.
16. Bechtold, J. K. and Matalon, M., *The dependence of the Markstein length on stoichiometry.* Combustion and Flame, 2001. 127(1-2): p. 1906-1913.
17. Bray, K. N. C. and Peters, N., *Laminar flamelets in turbulent flames*, in *Turbulent Reactive Flows*, P. A. Libby and A. Williams, Editors. 1994, Academic Press: London. p. 63-113.
18. Bradley, D., Gaskell, P. H., Sedaghat, A., and Gu, X. J., *Generation of PDFS for flame curvature and for flame stretch rate in premixed turbulent combustion.* Combustion and Flame, 2003. 135(4): p. 503-523.
19. Bray, K. N. C. and Cant, R. S., *Some appications of Kolmogorov's turbulence research in the field of combustion.* Proc R Soc Lond, 1991. A434: p. 217-240.
20. Muppala, S. P. R., Aluri, N. K., Dinkelacker, F., and Leipertz, A., *Development of an algebraic reaction rate closure for the numerical calculation of turbulent premixed methane, ethylene and propane/air flames for pressures up to 1.0 MPa.* Combustion and Flame, 2005. 140: p. 257-266.
21. Dinkelacker, F., Manickam, B., and Muppala, S. P. R., *Modelling and Simulation of Turbulent Methane/Hydrogen/Air Flames with an Effective Lewis Number Approach.* Combustion and Flame, 2009. (accpted).
22. Bray, K. N. C., Libby, P. A., and Moss, J. B., *Flamelet crossing frequencies and mean reaction rates in premixed turbulent combustion.* Combust. Sci. Technol., 1984. 41: p. 143-172.
23. Duclos, J. M., Veynante, D., and Poinsot, T., *A comparison of flamelet models for premixed turbulent combustion.* Combustion and Flame, 1993. 95: p. 101-117.
24. Kobayashi, H., Kawabata, Y., and Maruta, K., *Experimental Study on General Correlation of Turbulent Burning Velocity at High Pressure.* Proceedings of the Combustion Institute, 1998. 27: p. 941-948.
25. Muppala, S. P. R. and Dinkelacker, F., *Numerical modelling of the pressure dependent reaction source term for premixed turbulent methane/air flames.* Progress in Computational Fluid Dynamics, 2004. 4(6): p. 328-336.
26. Aluri, N. K., Muppala, S. P. R., and Dinkelacker, F., *Large-Eddy Simulation of Lean Premixed Turbulent Flames of Three Different Combustion Configurations using a Novel Reaction.* Flow Turbulence and Combustion, 2008. 80(2).
27. Chen, Y.-C. and Bilger, R. W., *Experimental investigation of three-dimensional flame-front structure in premixed turbulent combustion: II. Lean hydrogen/air Bunsen flames.* Combustion and Flame, 2004. 138(1-2): p. 155-174.
28. Matalon, M. and Matkowsky, B. J., *Flames as gas dynamic discontinuities.* Journal Fluid Mechanics, 1982. 124: p. 239-260.
29. Kolmogorov, A. N., Petrovsky, E. G., and Piskounov, N. S., *A study of the diffusion equation with a source term and its application to a biological problem.*, in *Dokl. Akad. Nauk SSSR*. 1937, (in Russian; English translation In: Pelc\'e P, editor. Dynamics of curved fronts. San Diego: Academic Press, 1988). Bjulleten' MGU, Moscow State University, USSR, Section A, .
30. Zeldovich, Y. B., *Flame propagation in a substance reacting at initial temperature.* Combustion and Flame, 1980. 39: p. 219-224.

31. Betev, A. S., Karpov, V. P., Lipatnikov, A., and Vardosanidze, Z. P., *Hydrogen combustion in engines and preferential diffusion effects in laminar and turbulent flames.* Archivum Combustionis, 1995. 15(3-4): p. 188-215.
32. Lipatnikov, A., in *Private Communication*.
33. Kido, H., Nakahara, M., and Nakashima, K., *A Study on the Local Flame Displacement Velocity of Premixed Turbulent Flames.* JSME International Journal Series B, 2005. 48(1): p. 164-171.
34. FLUENT, *Ansys Incorporated*, in *Canonsburg, PA, USA*